Synthesis of Ternary (Zinc-Cupper-Iron) Mixed Oxidenano Composite and its Biocompatibility Study

Sajid M. Mansoori
Department of Chemistry, Shri Vile Parle Kelavni Mandal's, Mithibai College of Arts, Chauhan Institute of Science & Amrutben Jivanlal College of Commerce and Economics (Autonomous)Ville-Parle (West), Mumbai-400056, Maharashtra, India.

Abstract: Metal oxide nanoparticle (MON) biofunctionalization has a significant impact on biomedical domains. Because of this, it is necessary to comprehend how MON interact with proteins before considering the material for a specific biomedical application. Chemical co-precipitation was used to create ZnO: CuO: Fe_2O_3 nanocomposits. UV spectroscopy, X-ray powder diffraction (XRD), Fourier transform infrared spectroscopy (FTIR), transmission electron microscopy (TEM), scanning electron microscopy (SEM), and EDAX were used to investigate the synthesised nanocomposites. The single-phase cubic structure was validated by FTIR and XRD. Protein interaction with prepared nanocomposite was carried out using circular dichroism. In addition to the Cu-O and Zn-O vibration modes, the FTIR spectra validate the coexistence of both phases and the distinctive vibration of ferrites atoms at tetrahedral and octahedral sites. Debye Scherrer's formula yielded a crystallite size of 23–28 nm, but SEM revealed that the nanoparticles were 10–30 nm in size. No change in protein conformation on binding with ZnO:CuO:Fe_2O_3 nanocomposites indicates that the BSA-ZnO:CuO:Fe_2O_3 nanocomposite system is biologically compatible. Designing optimised MON for various biomedical applications will benefit from the study.

Key words: metal oxide nanocomposites, protein interaction, BSA, biocompatible

1. Introduction

The unique properties of nanoparticles (NPs) have attracted a lot of interest because they may be useful in a wide range of applications. The application of nanomedicines and nanovaccines is being thoroughly studied, especially in the biomedical sector. However, nothing is known regarding the dangers of nanomaterial exposure and their biocompatibility [1-3]. Human exposure to nanomaterials can be purposeful, as in the case

of using consumer goods using nanotechnology, or unintentional, as in the case of occupational exposure. Although there are more and more research showing the negative effects of nanomaterials in in-vitro biological systems, it is not yet apparent if the information can be accurately extrapolated to forecast the negative consequences of nanotechnology on people [4-5].
The interactions between cells and nanoparticles are ultimately determined by the formation of a protein corona, which is the outcome of protein adsorption once the nanoparticles have entered the body. When NPs interact with proteins, they can cause physiological or conformational changes in the protein as well as disrupt its regular functioning, which can be harmful to the body. The intricacies of the interaction mechanism and the biological fate of NPs are provided by an in-vitro interaction investigation of proteins [6-7].

The phenomena of proteins interacting with metal oxide surfaces has drawn more attention since it is crucial in assessing whether metal oxide nano materials are biocompatible for use in medicine.
Maghemite (γ-Fe_2O_3) is frequently utilised for drug administration, bioimaging, and biosensing applications, as well as for its anticancer properties [8-9].

Energy transfer based on CuO NPs can be applied successfully to FRET-based biosensors and biomolecular recognition. Because the protein binding on the NP surface affects their cellular uptake and biodistribution, it is crucial to characterize them to study the efficacy and toxicology of NPs in the human body. The antibacterial and biocidal qualities of copper oxide (CuO) and its many biological uses have garnered a lot of interest [10-12]. Copper oxide (CuO), zinc oxide (ZnO), and iron oxide (Fe_2O_3) are examples of metal oxide nanoparticles that are perfect for biological applications due to their antibacterial and antifungal characteristics [13].

In the nano domain, zinc oxide (ZnO) is one of the metal oxides which, with sufficient biofunctionalization, can be employed in a variety of biomedical applications, such as antibacterial activity [14], drug transport [15], bioimaging [14], biosensor [10], and cell viability [13]. BSA's interactions with Ag [16], Au [17], ZnO [18-20], and TiO_2 [21] have been studied.
The compounds known as ternary metal oxides (TMOs) are made up of three distinct metal oxides. In recent years, these materials have drawn a lot of attention because of their special qualities and possible uses in a variety of industries, including biomedicine. New therapeutic and diagnostic tools can be developed by taking advantage of TMO-protein interactions[22].
ZnO:CuO:Fe_2O_3 nanocomposites have garnered a lot of attention due to their unique

properties and applications in the biomedical sector. Protein-nanocomposites interactions are key to understanding their toxicity, biocompatibility, and potential applications. The complex interactions between ZnO:CuO:Fe_2O_3 nanocomposites and proteins need to be better understood in order to facilitate the development of novel applications and ensure the safe usage of these materials. More investigation is required to completely comprehend the intricate relationships between TMOs and proteins in order to guarantee the safe use of TMO-based products and to support the creation of novel applications [23].

2. Materials and methods:

The following materials were obtained from S.D. Fine Chem Limited: zinc sulphate heptahydrate ($ZnSO_4 \cdot 7H_2O$, 99%), sodium hydroxide (NaOH), ethanol, crystal violet, cupric nitrate trihydrate ($Cu(NO_3)_2.3H_2O$, 99.5%), and ferrous ammonium (II) sulphate heptahydrate ($FeSO_4 \cdot 7H_2O$, 99%). All analytical-grade chemical reagents were utilised without additional purification.

Synthesis of ZnO: CuO: Fe_2O_3 nanocomposite

$Cu(NO_3)_2.3H_2O$, $ZnSO_4.7H_2O$, and $Fe(NH_4)SO_4.7H_2O$ dissolved in deionised water with 1:3:4, ratios of CuO, ZnO, and Fe_2O_3 were used to create a ZnO:CuO:Fe_2O_3 nanocomposite using the co-precipitation method. The precipitation of metal ion hydroxides by concentrated sodium hydroxide. The precipitates underwent filtering, multiple distilled water washes, and a 24-hour electrical oven drying process at 110 ^oC. In a tube furnace, the dehydrated samples were calcined for six hours at 500 ^oC (24, 25).

3. Structural Characterization

To measure the optical absorption spectra between 300 and 800 nm, the Systronic UV-2203 UV-Vis spectrophotometer was utilised. The Schimadzu XRD-7000 and CuKα were used to capture the X-ray diffraction pattern in the 2theta 10nm to 80nm region, using a wavelength of light (λ = 0.15406 nm). Particle size and elemental analysis of the generated A Scanning Electron Microscope with Energy Dispersive X-Ray Analysis (JEOL-JSM-6360A) was used to evaluate the nanocomposites. FTIR analysis was performed in a KBr matrix using a Perkin Elmer (RFPC-5301) with a range of 500–4000 cm^{-1}. The TEM (PHILIPS-CM 200) was used to observe the produced nanocomposites in order to determine their precise morphologies [25-26].

4. Denaturation studies

Using the Jasco-815 CD spectrometer, CD spectra were acquired at room temperature in the far UV (180-260 nm) and near UV (260-360 nm) regions. Over a 1 cm route length, the BSA concentration was 15×10^{-6} mol dm^{-3} in the near UV region and 0.3×10^{-6} mol dm^{-3} in the

far UV zone. Throughout the experiment, the nitrogen gas was purged. The molar ellipticity [θ] is displayed against the appropriate wavelength in the CD spectrum [27].

4. Results and Discussion

a. UV- Specroscoscopy

$ZnO:CuO:Fe_2O_3$ nanocomposite show strong visible light absorption at 500nm(fig 1)

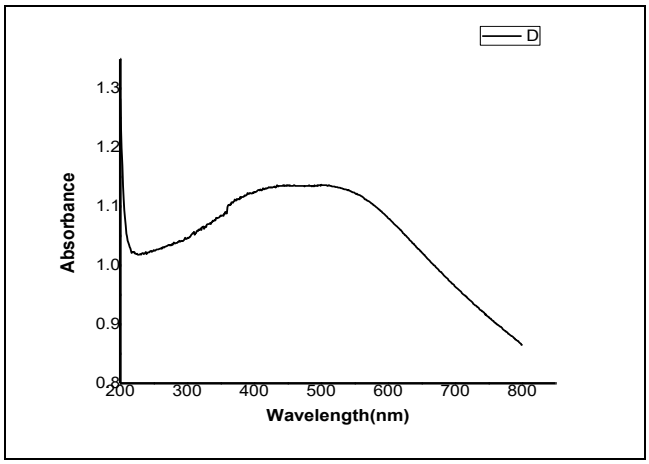

Fig 1: a) $ZnO:CuO:Fe_2O_3$ nanocomposite UV absorption spectrum

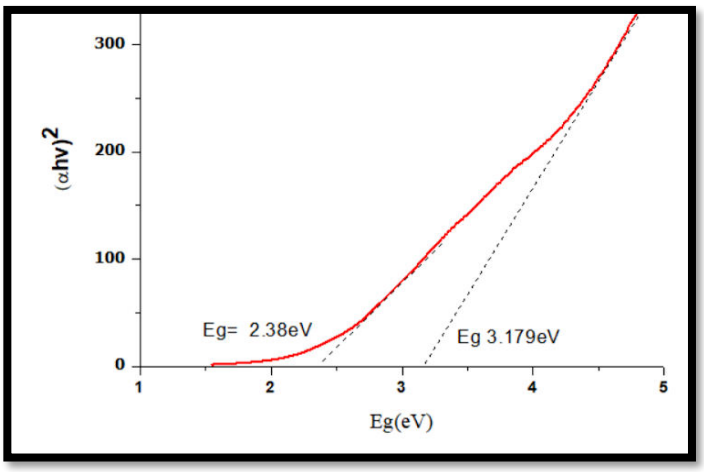

Figure 2: The $ZnO:CuO:Fe_2O_3$ nanocomposites' band gap energy curves

The direct and indirect band gap energy determine from the plot of $(\alpha h\upsilon)^2$ versus Eg (Fig 2) by extrapolating the curve's linear part to the energy axis for as-synthesized $ZnO:CuO:Fe_2O_3$ nanocomposite. The direct band gap is 3.17eV, and the indirect band gap is 2.38eV. Therefore, it was expected that the $ZnO:CuO:Fe_2O_3$ nanocomposite possessed comparatively good semiconductor properties and possessed photocatalytic activity in the visible region. [28-29].

b. XRD

X-Ray Diffraction Studies shows the major diffraction peaks are between 15° and 65° (2 θ)

(figure 3) .The 2-θ values of the diffraction peak are 29.96°, 35.31°, 56.75° and 62.30° corresponded to the (220), (311), (222), (220), (333) and (440) planes of α- Fe_2O_3 nanoparticles respectively (JCPDS 36-1451). The peak at 2θ = 29.96° the (220) plane of Fe_3O_4. Hexagonal wurtzite structure of ZnO nanoparticle belong to the (JCPDS data card No. 79-2205). The monoclinic structure of CuO is confirmed by the well-developed peaks in the nanocomposite's XRD pattern at 2θ = 18.23°, 38.71°, 42.9°, 53.3°, and 59.36°, which are caused by the (1 1 0), (1 1 1), (1 1 1), (1 1 2), (2 0 2), (1 1 2), (0 2 0), (2 0 2), (1 1 3), and (0 2 2) planes, respectively (JCPDS data card No. 89-2529). Absence of other copper peaks in the XRD spectrum indicates that air oxidation occurs when annealed at 5000 C. The peaks at 2θ = 18.2° ascribed to the (200) planes of CuO are shown to grow in intensity with the concentration of CuO. this suggest that oxides combine inter grain coupling instead of intra granular coupling. The diffraction peaks at 2θ values of 17.65, 29.96, 35.35, 36.95, 42.95, 56.7596 and 62.30 corresponded to the (111), (220), (311),(222), (220), (422), (333) and (440) ZnO nanoparticle planes that are hexagonal, respectively (JCPDS 36-1451).[25-30]

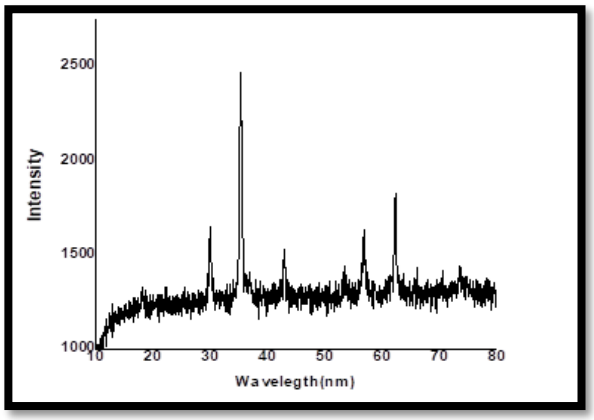

Figure 3: XRD spectra of ZnO:CuO:Fe_2O_3 nanocomposite

According to Debye-Scherer's formula, the size of a crystalline particle (31).

Average particle size (D) $= \frac{0.9 \times \lambda}{\beta \times \cos\theta}$

Where, D, λ, β, and θ stand for crystalline particle size, X-ray wavelength, diffraction angle, and diffraction peak widening, respectively.

Table 1: Particle size of ZnO: CuO:Fe_2O_3 nanocomposite

2theta (2 θ)	θ /2	Θ in radians	fwhm	d in radians	d particle size A°	particle size nm
35.315	17.66	0.3081815	0.3591	0.006267	232.1659	23.21659
62.3095	31.15	0.5437530	0.3364	0.005871	275.9564	27.59564
29.9626	14.98	0.2614730	0.3448	0.006018	238.5097	23.85097

The particle size obtained using Debye-Scherer's formula is between 20-30nm as mention in

table 1.

c. FTIR Spectra

The ZnO: CuO: Fe_2O_3 nanocomposite's transmittance spectra are shown in Figure 4. A wide peak in the FTIR spectrum at about 550 cm^{-1} corresponds to the M-O vibrational mode at the tetrahedral site . Fe–O, Cu–O, and Zn–O stretching vibrations overlap in the 400–800 cm^{-1} range. According to recent research (27–29), the Zn–O stretching band and the Cu–O stretching band in the monoclinic phase are found in the 400–660 and 430–610 cm^{-1} areas, respectively, whereas the distinctive peaks of Fe–O in Fe_3O_4 are located at 570 and 375 cm^{-1}. 1114-1128 cm^{-1} is equivalent to 1000-1250 cm^{-1} of Cu-O stretching vibration. The peak at 1435 cm^{-1} is caused by the stretching vibration of C=O [25-26, 32-35].

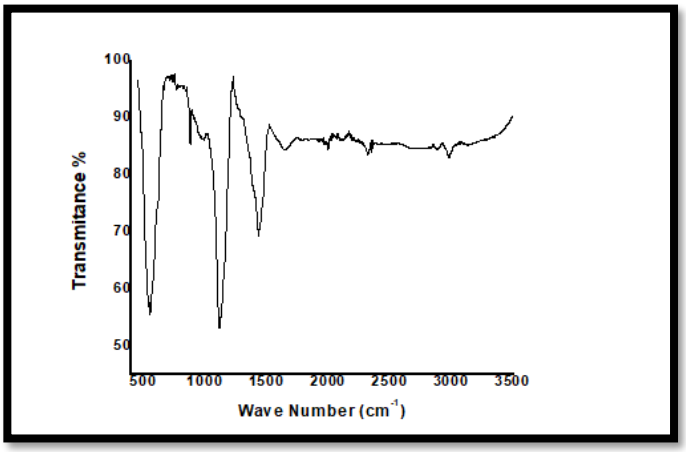

Figure 4: FTIR spectra of CuO:ZnO:Fe_2O_3 nanocomposite

d. SEM and EDAX:

The aggregated morphology of nanocomposites has mixture of nano particle with grain size around 10 to 40 nm as shown in fig. 5a. However, EDAX spectra (Fig. 5b) confirms the presence of the expected chemical element on the samples. The prepared ZnO:CuO:Fe_2O_3 nanocomposites are in agreement with EDAX and XRD results.

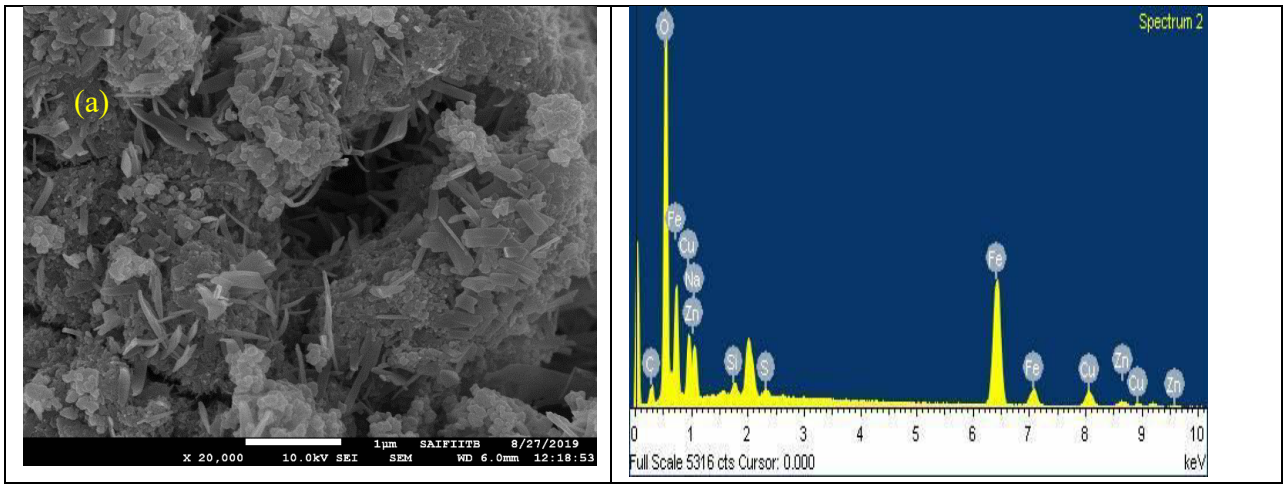

Figure 5: a)FESEM of CuO:ZnO:Fe_2O_3 nanocompositeb) EDAX of CuO:ZnO:Fe_2O_3 nanocomposite

The EDAX clearly confirm the presence of Cu, Zn and Fe , oxygen and traces of Na, sulphur and Si.

The ternary nanocomposite ZnO: CuO:Fe_2O_3 EDX analysis is shown in Figure 5b, which also shows the mass and atomic percentages of the various components. These value percentages are summarised for convenience in the attached table. iron (Fe) and oxygen (O) have greater atomic percentages and masses, which suggests that they predominate in the composition as shown in table 2.

Table 2: Weight and atomic percentage of CuO:ZnO:Fe_2O_3 nanocomposite

Element	Weight%	Atomic%
C K	5.02	11.81
O K	30.47	53.83
Na K	3.13	3.85
Si K	0.83	0.84
S K	0.49	0.44
Fe K	42.05	21.29
Cu L	13.33	5.93
Zn L	4.68	2.02
Totals	100.00	

The synthesis process or the type of raw materials employed may be responsible for this.

e. TEM

Transmission Electron Microscopic Studies of ZnO:CuO:Fe_2O_3 nano composite shows Rod like structure of CuO, Spherical Fe_2O_3 and wurtzite shape of ZnO in fig. 6 TEM images

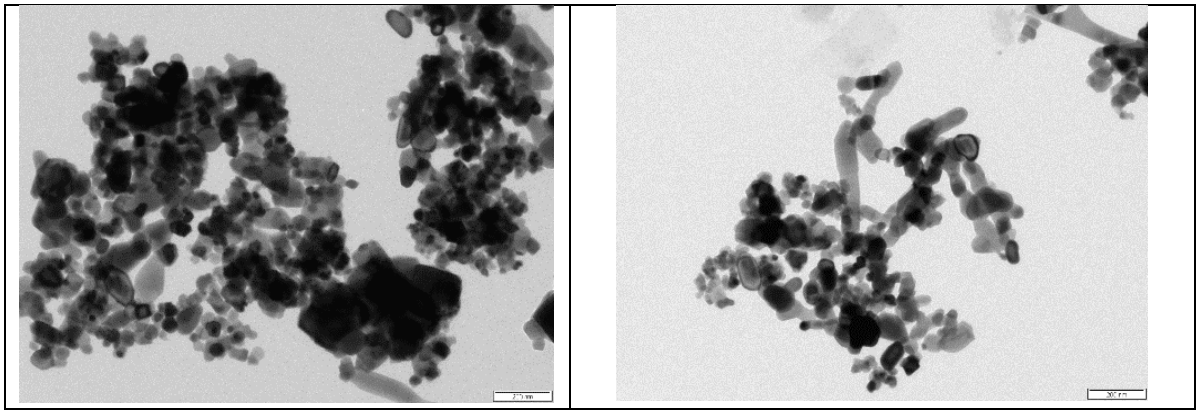

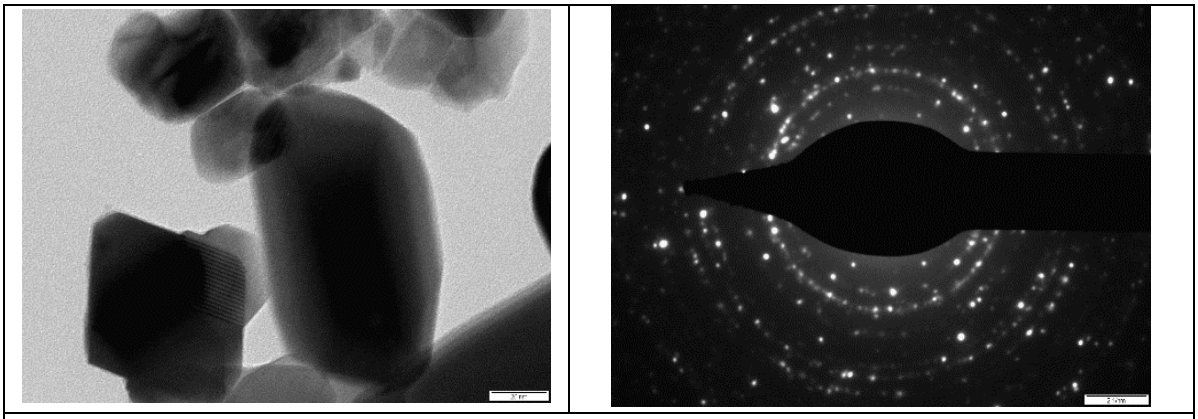

Figure 6: TEM images of nanocomposite a) 200nm b) 50nm c) 20nm d) 20 nm

f. Circular dichroism spectroscopy

Conformation of proteins in aqueous solution can be studied by Circular dichroism spectroscopy. Biological activity of the proteins is affected by conformational changes in its structure. It provides information whether protein is denatured on not when they are interacted with nanoparticles. The BSA spectra (in Figure 7) were captured both with and without the nanocomposite. The near UV signal indicates that BSA's tertiary structure doesn't change over the course of the system.

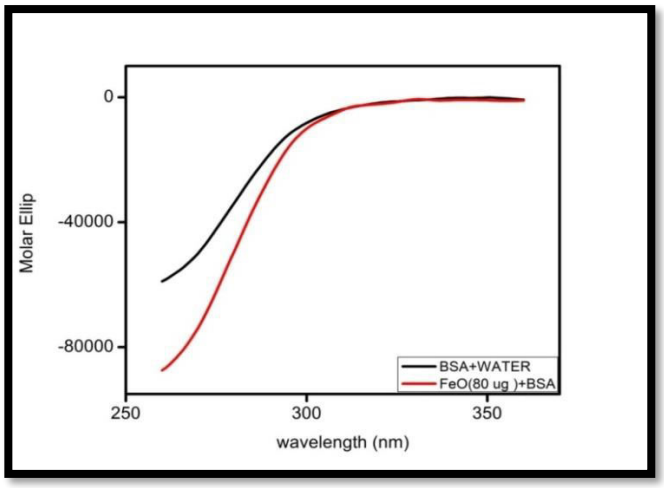

Figure 7: Spectra of BSA near UV both with and without ZnO:CuO:Fe_2O_3 nanocomposites. No change in protein conformation on binding with Nanocomposite indicates that the BSA-Nanocomposite system is biologically compatible.

5. Conclusions

ZnO:CuO:Fe_2O_3 nanocomposites were synthesised using a simple co-precipitation technique. This sample's FTIR spectrum reveals the existence of functional groups linked to metal oxides. ZnO:CuO:Fe_2O_3 nanocomposites were detected by the prominent peaks in the XRD results, which also showed that the generated sample was nanosized. TEM image of Nanocomposite shows rod like, spherical, wurtzite shape of crystal of CuO, Fe_2O_3 and ZnO

respectively. No change in protein conformation on binding with ZnO:CuO:Fe_2O_3 nanocomposites indicates that the BSA- ZnO:CuO:Fe_2O_3 nanocomposites system is biologically compatible. Further protein interaction with other metal oxide nanocomposite can be studied for better understanding of BSA-metal oxide nanocomposite interaction and their biocompatibility.

6. **Acknowledgment**s: The author acknowledge the IIT-Bombay for SEM/EDAX/TEM analysis and University of Mumbai for FTIR and XRD and circular dichroism.

7. **Conflicts of Interest:** The authors declare that they have no known competing financial interests or personal relationships that could have influenced the work reported in this paper.

References

1. Aflori, M. Smart Nanomaterials for Biomedical Applications, A Review. Nanomaterials, 11, 396. (2021).
2. Cardoso, V.; Francesko, A.; Ribeiro, C.; Bañobre-López, M.; Martins, P.; Lanceros-Mendez, S. Advances in Magnetic Nanoparticles for Biomedical Applications. Adv. Health Mater. 7, 1700845. (2018).
3. Seaberg, J.; Montazerian, H.; Hossen, N.; Bhattacharya, R.; Khademhosseini, A.; Mukherjee, P. Hybrid Nanosystems for Biomedical Applications. ACS Nano, 15, 2099–2142. (2021)
4. Naskar, A.; Kim, K.-S. Potential Novel Food-Related and Biomedical Applications of Nanomaterials Combined with Bacteriocins. Pharmaceutics, 13 86. (2021)
5. Hosseinkhani, H.; Domb, A.J. Biodegradable polymers in gene-silencing technology. Polym. Adv. Technol., 30, 2647–2655. (2019),
6. S. Prasanth, D. Rithesh Raj, T.V. Vineeshkumar, C. Sudarsanakumar, Spectroscopic exploration of interaction between PEG-functionalized Ag_2S nanoparticles with bovine serum albumin, Chemical Physics Letters (2018),
7. A. E. Nel, L. Mädler, D. Velegol, T. Xia, E. M. V. Hoek, P. Somasundaran, F. Klaessig, V. Castranova, M. Thompson, Understanding biophysicochemical interactions at the nano–bio interface, Nat. Mater. 8, 543-557. (2009).
8. Naskar, A., Lee, S., Ko, D., Kim, S., Kim, K., Bovine Serum Albumin-Immobilized Black Phosphorus-Based-Fe_2O_3 Nanocomposites: A Promising Biocompatible Nanoplatform, Biomedicines, 9, 858. (2021),
9. Qinqin Yang, Jiangong Liang, Heyou Han, Probing the Interaction of Magnetic Iron Oxide Nanoparticles with Bovine Serum Albumin by Spectroscopic Techniques ,J. Phys. Chem. B., 113 , 10454–10458. (2009).
10. Naskar A, Lee S, Ko D, Kim S, Kim KS. Bovine Serum Albumin-Immobilized Black Phosphorus-Based γ-Fe_2O_3 Nanocomposites: A Promising Biocompatible Nanoplatform. Biomedicines, 22, 9(8) 858. (2021).

11. Nations, S., Long, M., Wages, M., Maul,J.D., Theodorakis, C. W., & Cobb, G. P. Subchronic and chronic developmental effects of copper oxide (CuO) nanoparticles on Xenopus laevis. Chemosphere, 135, 166–174, (2015).
12. Grigore, M. E., Biscu, E. R., Holban, A. M., Gestal, M. C., &Grumezescu, A. M, Methods of synthesis, properties and biomedical applications of CuO nanoparticles. Pharmaceuticals, 9 ,75, (2016).
13. Laurent, S.; Forge, D.; Port, M.; Roch, A.; Robic, C.; Vander Elst, L.; Muller, R. N., Chem. ReV. 108, 2064, (2008).
14. Nikolova M.P., Chavali M.S. Metal Oxide Nanoparticles as Biomedical Materials. Biomimetics, 5, 27, (2020).
15. Couto D., Freitas M., Carvalho F., Fernandes E. Iron Oxide Nanoparticles, An Insight into their Biomedical Applications. Curr. Med. Chem., 22, 1808–1828, (2015).
16. Dasgupta N., Ranjan S., Patra D., Srivastava P., Kumar A., Ramalingam C., Bovine serum albumin interacts with silver nanoparticles with a “side-on” or “end on” conformation. Chem. Interact. ,253, 100–111, (2016).
17. Matei I., Buta C.M., Turcu I.M., Culita D., Munteanu C., Ionita G. Formation and Stabilization of Gold Nanoparticles in Bovine Serum Albumin Solution. Molecules. 24:3395, (2019).
18. Naskar A., Khan H., Bera S., Jana S. , ,Soft chemical synthesis, characterization and interaction of ZnO graphene nanocomposite with bovine serum albumin protein. J. Mol. Liq., 237, 113–119, (2017).
19. G. Simonelli, E. L. Arancibia, Effects of size and surface functionalization of zinc oxide (ZnO) particles on interactions with bovine serum albumin (BSA), J. Mol. Liq. 211, 742-746, (2015).
20. N. P. Sasidharan, P. Chandran, S. S. Khan, Interaction of colloidal zinc oxide nanoparticles with bovine serum albumin and its adsorption isotherms and kinetics, Colloids Surf. B 102 ,195-201,(2013).
21. Ranjan S., Dasgupta N., Srivastava P., Ramalingam C. A spectroscopic study on interaction between bovine serum albumin and titanium dioxide nanoparticle synthesized from microwave-assisted hybrid chemical approach. J. Photochem. Photobiol. B Biol. 161, 472–481, (2016).
22. Priya Gaikwad, Nidhi Tiwari, Rajanish Kamat, Sagar M. Mane, Shriniwas B. Kulkarni,A comprehensive review on the progress of transition metal oxides materials as a supercapacitor electrode, Materials Science and Engineering: B, 307, 117544, (2024).
23. Sahoo S, Wickramathilaka KY, Njeri E, Silva D, Suib SLA review on transition metal oxides in catalysis. Front Chem. 17(12), 374878, (2024).
24. Abdelghani Serouti, et albiogenic ZnO/CuO/Fe_2O_3nanocomposite:a ground breaking approach for enhanced degradation capabilities and reusability in dye removal applications , arabian journal for science and engineering, 49, 753–764, (2024).

25. A. Taufik, R. Saleh, Synthesis of iron (II, III) oxide/zinc oxide/copper (II) oxide (Fe_3O_4/ZnO/CuO) nanocomposites and their photosonocatalytic property for organic dye removal, J. Colloid Interface Sci, 491, 27–36,(2017).
26. Sajid M. Mansoori, Ramesh S. Yamgar and Shreemant V. Rathod, Synthesis of Zinc-Copper-Iron(II, III) Oxide Nanocomposites and their Photocatalytic Efficiency for Crystal Violet Degradation, Malaysian Journal of Chemistry, 23(1), 15-23, (2021).
27. Amit Kumar Bhunia, Satyajit Saha, CuO Nanoparticle-Protein Bioconjugate: Characterization of CuO Nanoparticles for the Study of the Interaction and Dynamic of Energy Transfer with Bovine Serum Albumin, BioNanoScience ,**10**, 89–105,(2020).
28. Ahmad A. Mohd, Setapar, S. H., Chuong, C. S., Khatoon A., Wani, W. A., Kumar, R., Rafatullah, M. Recent advances in new generation dye removal technologies: Novel search for approaches to reprocess wastewater. RSC Adv, 5, 30801–30818. 6. (2015).
29. Chatterjee, D. and Dasgupta, S. Visible light induced photocatalytic degradation of organic pollutants, J PhotochemPhotobiol C – Photochem Rev., 6,186–205, (2005).
30. Volkan Eskizeybeka, et. al. Preparation of the new polyaniline/ZnO nanocomposite and its photocatalytic activity for degradation of methylene blue and malachite green dyes under UV and natural sun lights irradiations, Applied Catalysis B: Environmental, 119-120, 197– 206, (2012).
31. Ardiansyah Taufik and Rosari Saleh Synergistic effect between ternary iron–zinc copper mixed oxides and graphene for photocatalytic water decontamination, Ceramics International, 43, 3510–3520, (2017).
32. Joshi, B. N., Yoon, H., Na, S., Choi, J. Y, Yoon, S. S. (2014) Enhanced photocatalytic performance of graphene–ZnO nanoplatelet composite thin films prepared by electrostatic spray deposition, Ceram. Int., 40, 3647–3654, (2014).
33. Yang, C., Cao, X., Wang, S., Zhang, L., Xiao, F., Su, X., Wang, J. Complex-directed hybridization of CuO/ZnO nanostructures and their gas sensing and photocatalytic properties, Ceram. Int., 41, 1749–1756, (2015).
34. Zhang, Q., Zhang, K., Daguo Xu, Yang, G., Huang, H., Nie, F., Liu, C., Yang, S. Synthesis, Characterization, growth mechanisms, fundamental properties, and applications, Prog. Mater. Sci., 60, 208–337,(2014).
35. Ghosh, A., Mondal, A. Fabrication of stable, Fabrication of stable, efficient and recyclable p-CuO/n-ZnO thin film heterojunction for visible light driven photocatalytic degradation of organic dyes, Mater. Lett, 164, 221–224, (2016).
36. Saravanan, R., Karthikeyan, S., Gupta, V. K., Sekaran, G., Narayanan, V., Stephen, A. Enhanced photocatalytic activity of ZnO/CuO nanocomposite for the degradation of textile dye on visible light illumination, Mater. Sci. Eng., C. 33, 91–9, (2013).